Inorganic Chemistry

Article

pubs.acs.org/IC

Lanthanide Complexes Based on β-Diketonates and a Tetradentate Chromophore Highly Luminescent as Powders and in Polymers

Eugen S. Andreiadis,[†] Nicolas Gauthier,[†] Daniel Imbert,[†] Renaud Demadrille,[‡] Jacques Pécaut,[†] and Marinella Mazzanti*,[†]

[†]CEA-Grenoble, INAC, SCIB, Laboratoire de Reconnaissance Ionique et Chimie de Coordination, UMR-E 3 CEA-UJF, 38054 Grenoble Cedex 9, France

[‡]CEA Grenoble, INAC, SPrAM, Laboratoire d'Electronique Moléculaire, Organique et Hybride, UMR 5819 CEA-CNRS-UJF, 38054 Grenoble, France

Supporting Information

ABSTRACT: A new type of octacoordinated ternary β-diketonates complexes of terbium and europium has been prepared using the anionic tetradentate terpyridine-carboxylate ligand (**L**) as a sensitizer of lanthanide luminescence in combination with two β-diketonates ligands 2-thenoyltrifluoroacetyl-acetonate (tta^-) for Eu^{3+} and trifluoroacetylacetonate ($tfac^-$) for Tb^{3+}. The solid state structures of the two complexes $[Tb(\mathbf{L})(tfac)_2]$ (**1**) and $[Eu(\mathbf{L})(tta)_2]$ (**2**) have been determined by X-ray crystallography. Photophysical and ^1H NMR indicate a high stability of these complexes with respect to ligand dissociation in solution. The use of the anionic tetradentate ligand in combination with two β-diketonates ligands leads to the extension of the absorption window toward the visible region (390 nm) and to high luminescence quantum yield for the europium complex in the solid state (Φ = 66(6)%). Furthermore, these complexes have been incorporated in polymer matrixes leading to highly luminescent flexible layers.

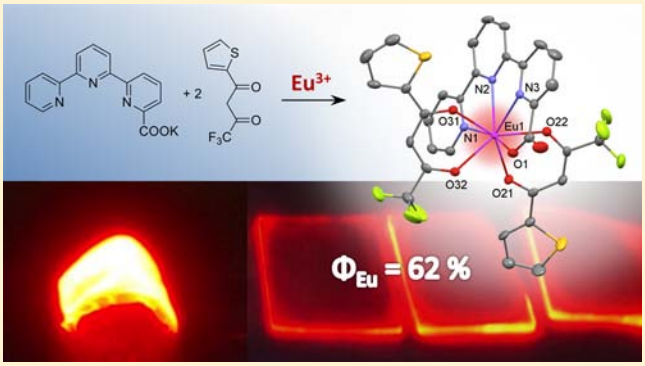

INTRODUCTION

In recent years, there has been a renewal of interest in luminescent β-diketonate complexes of lanthanides because their attractive luminescent properties (high quantum yields, narrow band emission) and their processability can find use in a wide range of applications.[1−5] Notably, ternary complexes [Ln(β-diketonate)$_3$L] containing an additional bidentate or tridentate chromophore are gaining increasing attention for technological application such as organic emitting layers in light-emitting diodes (OLED)[6−10] and wavelength conversion materials in solar cells.[4,11−16] Applications in biological imaging have also been reported for the two-photon sensitized luminescence[17] of ternary diketonate complexes.[18−20]

Typically tris-diketonate complexes prepared in non anhydrous solvents present two water molecules in the first coordination sphere that lead to the nonradiative deactivation of the lanthanide luminescence emission. Highly luminescent homoleptic and heteroleptic β-diketonate complexes of europium have been obtained by replacing the coordinated water molecules in [Eu(β-diketonate)$_3$(H$_2$O)$_2$] with neutral N- or O-donor ligands[2,21−23,14,22,24−33] or with a fourth diketonate ligand.[34,35] Such ligands prevent the nonradiative deactivation of the luminescence by removing the O−H quenching and function as an additional sensitizer allowing the fine-tuning of the luminescence properties.

β-Diketonate ligands are known to be quite resistant with respect to ligand dissociation,[2,36,37] but neutral O- or N-donor ligands are more easily displaced by protic solvents.[26] Thus, the handling of ternary complexes containing a neutral sensitizer in nonanhydrous solvents might result in a decrease of the overall luminescence quantum yields.

Recent reports show that monoanionic and dianionic tridentate or tetradentate heterocyclic N-donor ligands are very efficient sensitizers of lanthanide luminescence and form robust mononuclear lanthanide complexes.[38−44] Surprisingly such ligands have not been used in the preparation of ternary β-diketonate complexes.

Here we report a new type of ternary lanthanide complexes of Eu(III) and Tb(III) built from the self-assembly of a tetradentate monoanionic ligand (2,2′:6′,2″-terpyridine-6-carboxylate) (**L**) and two β-diketonate ligands around the lanthanide ions (Scheme 1). 2-Thenoyltrifluoro-acetylacetonate (tta^-)[44,45] has been used for the effective sensitization of europium luminescence in combination with **L**.[45,46] For the Tb(III) ion the ligand **L** is used together with trifluoroacetylacetonate ($tfac^-$) which presents a triplet state energy level suitable for energy transfer toward the $^5D_4$ state of terbium.[47]

Received: October 5, 2013
Published: November 21, 2013

Scheme 1. [Tb(L)(tfac)$_2$] (1) and [Eu(L)(tta)$_2$] (2) Complexes

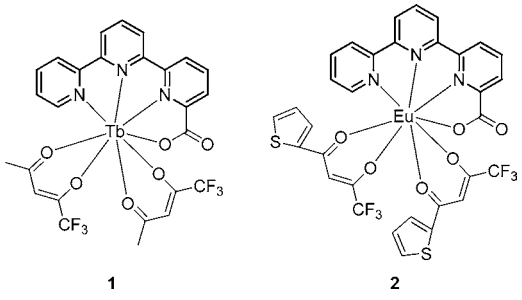

1 2

The resulting octacoordinated [Ln(**L**)(β-diketonates)$_2$] (Ln = Tb **1**; Ln = Eu, **2**) complexes are robust with respect to ligand dissociation and highly luminescent with an excitation window extending close to the visible range (390 nm). We report the structure and the photophysical properties of these complexes in the solid and solution state. We also describe the incorporation of [Eu(**L**)(β-diketonates)$_2$] in two different polymetric matrixes, poly(methylmethacrylate) (PMMA), and poly(vinyl-acetate) (PVA), to afford highly luminescent and flexible materials. The efficient incorporation of luminescent lanthanide complexes in a polymer matrix with good mechanical properties, lightweight, transparency, and low temperature process ability is crucial in potential technological applications such as OLED and photovoltaic devices.[4,7,12,23,48,49]

EXPERIMENTAL SECTION

General Procedure. Anhydrous tetrahydrofuran, trifluoroacetylacetone (tfacH), and 2-thenoyltrifluoroacetone (ttaH) were purchased from Aldrich and used without any purification. Lanthanide triflate salts (EuOTf$_3$·xH$_2$O with x = 0.15−0.3) were purchased from Aldrich and titrated for metal content before use, in the presence of EDTA and xylene orange.[50] ^{1}H and ^{13}C NMR spectra were recorded at 298 K for characterization purposes on a Bruker Advance 200 and a Varian Unity 400 spectrometers. Chemical shifts are reported in ppm and were referenced internally to the residual solvent resonance. Mass spectra were run on a Thermo Scientific LXQ mass spectrometer equipped with an electrospray source. Thickness measurements were performed using a profilometer XP2 (Ambios Technology). Elemental analyses were performed by the Service Central d'Analyses of CNRS (Vernaison, France).

X-ray Crystallography. Diffraction data for both complexes were collected using an Oxford Diffraction Xcalibur S Kappa area detector four-circle diffractometer, controlled by the Oxford Diffraction CrysAlis CCD software (Mo−Kα radiation, graphite monochromator, λ = 0.71073 Å).[51] To prevent evaporation of cocrystallized solvent molecules, the crystals were coated with a light hydrocarbon oil. Unique intensities detected on all frames using the Oxford-diffraction Red program were used to refine the values of the cell parameters. The substantial redundancy in data allows empirical absorption corrections to be applied using multiple measurements of equivalent reflections with the ABSPACK Oxford-diffraction program.[52] Space groups were determined from systematic absences. The structures were solved by direct methods using the SHELXTL 6.14 package,[53] and all the atoms, including hydrogen atoms, were found by difference Fourier syntheses. All non-hydrogen atoms were anisotropically refined on F. Hydrogen atoms were refined isotropically for the tfa$^-$ ligand except where the hydrogens of the disordered positions were fixed in ideal position and refined with a riding model. For the tta$^-$ ligand, all hydrogen atoms were fixed in ideal position and refined with a riding model. Experimental details for X-ray data collections are given in Supporting Information, Tables S1 and S2.

Photophysical Measurements. Absorption spectra were recorded in 1 cm quartz cells on a Cary 50 Probe UV−vis spectrophotometer. Emission, excitation spectra, and lifetimes were recorded by using a Perkin-Elmer LS-50B and a modular Fluorolog FL 3-22 spectrometer from Horiba-Jobin Yvon-Spex equipped with a double grating excitation monochromator and a iHR320 imaging spectrometer fitted with a Hamamatsu R928P photomultiplier. All spectra were corrected for detection and optical spectral response (instrumental functions) of the spectrofluorimeters. Quartz cells with an optical path of 1 cm and quartz capillaries 4 mm in diameter were used. Phosphorescence lifetimes were measured in time-resolved mode and are the averages of three independent measurements that were taken by monitoring the decay at the maxima of the emission spectra. The signals were analyzed with the Origin Pro software.[54]

The quantum yields were determined at room temperature through an absolute method using an integrating sphere from GMP S.A. (Switzerland) coupled to the spectrofluorimeter. The values reported are the average of three independent determinations for each sample. The absolute quantum yields were calculated using the following expressions:

$$\Phi = \frac{E_c}{L_a - L_c} = \frac{E_c}{L_a \cdot \alpha} \qquad \alpha = \frac{L_a - L_c}{L_a} \tag{1}$$

where E_c, L_c, and L_a are the emission spectra of the sample, the excitation wavelength of the sample, and the excitation wavelength of the reference, respectively.

Preparation of the Solutions. The [Gd(**L**)$_2$]K complex was prepared in situ by adding 0.05 mmol of KOH (1 M in methanol) to a suspension of HL (0.05 mmol) in methanol (5 mL) stirred at room temperature and then adding 0.025 mmol of a titrated solution of gadolinium triflate in methanol.

The [Tb(**L**)(tfac)$_2$] and [Eu(**L**)(tta)$_2$] solutions for UV−visible and luminescence measurements in methanol and tetrahydrofuran (THF) were prepared by dissolving a correct amount of the dried complexes. The concentrations used were in the range 1.00−3.96 × 10^{-5} M.

Synthesis. The 6,2′:6′,2″-terpyridine-2-carboxylic acid H**L** was synthesized according to the reported procedure, by oxidation of the 6-methyl-2,2′:6′-2″-terpyridine precursor with selenium dioxide in pyridine according to the reported procedure.[55]

[Tb(L)(tfac)$_2$] (1). A suspension of ligand H**L** (0.14 g, 0.5 mmol) in methanol (2 mL) was reacted with a 1 M KOH solution in methanol (0.5 mL, 0.5 mmol) to give a clear solution. A solution of terbium triflate (0.306 g, 0.5 mmol) in methanol (2 mL) was then added. After a few minutes, trifluoroacetylacetone (tfac, 122 μL, 1.0 mmol) in KOH (1 mL, 1 mmol, 1 M solution in methanol) was added to the resulting yellow solution. The reaction mixture was stirred at room temperature for 1 h, then the solvent was evaporated and the complex extracted with dichloromethane. The organic phase was washed with water, dried over Na_2SO_4, and the solvent was evaporated to give 0.292 g of white powder (78%). The complex was dried under vacuum and stored under argon.

^{1}H NMR (400 MHz, $CDCl_3$, 298 K): δ ppm 117.16 (br, 2H, H$_b$), 13.58 (br, 6H, H$_a$), −4.07 (br, 1H), −8.29 (br, 1H), −14.05 (br, 1H), −16.04 (br, 1H), −21.02 (br, 1H), −24.98 (br, 1H), −30.09 (br, 1H), −49.59 (br, 1H), −52.37 (br, 1H), −116.7 (br, 1H). Elemental analysis calcd(%) for $C_{26}H_{18}F_6N_3O_6Tb$·0.5 CH_2Cl_2: C 40.61, H 2.44, N 5.36; found: C 40.52, H 2.26, N 5.61.

Recrystallization by slow evaporation of a solution of the complex **1** in methanol afforded crystals of **1**·MeOH suitable for X-ray diffraction.

[Eu(L)(tta)$_2$] (2). A suspension of ligand H**L** (0.12 g, 0.435 mmol) in methanol (2 mL) was reacted with a 1 M KOH solution in methanol (0.435 mL, 0.435 mmol) to give a clear solution. A solution of europium triflate (0.26 g, 0.435 mmol) in methanol (2 mL) was then added. After few minutes, a solution of thenoyltrifluoroacetone (tta, 0.193 g, 0.87 mmol) in KOH (1 M solution in methanol, 0.87 mL, 0.87 mmol) was added. The reaction mixture was stirred at room temperature for 1 h; then the solvent was evaporated, and the complex extracted with dichloromethane. The organic phase was washed with water, dried over Na_2SO_4, and the solvent was evaporated to afford **2**

dx.doi.org/10.1021/ic402523v | Inorg. Chem. 2013, 52, 14382−14390

as a white-cream powder (97%). The complex was dried under vacuum and stored under argon.

^{1}H NMR (400 MHz, MeOD, 268 K): δ ppm 13.59 (br, 1H, H_{10}), 9.49 (br, 1H, H_5), 9.32 (br, 1H, H_6), 9.09 (br, 1H, H_4), 8.82 (br, 1H, H_8), 8.62 (br, 1H, H_7), 8.19 (br, 1H, H_2), 7.95 (br, 1H, H_9), 7.85 (br, 1H, H_3), 7.66 (br, 1H, H_1), 6.69 (br, 2H, H_{11}), 5.87 (br, 2H, H_{12}), 4.67 (br, 2H, H_{13}), 1.42 (br, 2H, H_{14}). ES$^+$-MS m/z (carried out in the presence of added K^+ ions): 909.9 $[Eu(L)(tta)_2]K^+$. Elemental analysis calcd (%) for $C_{32}H_{18}EuF_6N_3O_6S_2{\cdot}CH_2Cl_2$: C 41.48, H 2.11, N 4.40; found: C 41.63, H 2.22, N 4.52.

Recrystallization by slow evaporation of a solution of the complex **2** in methanol afforded crystals of **2** suitable for X-ray diffraction.

Film Preparation. Poly(methylmethacrylate) (PMMA) and polyvinylacetate (PVA) doped films of $[Eu(\mathbf{L})(tta)_2]$ were prepared by dissolving purified PMMA or PVA pellets in THF (low molecular weight, 5% or 10% w/w, respectively) in the presence of the desirable concentration of **2**. PMMA doped films were obtained by spin-coating on borosilicate substrates (17.5 × 20 mm) using the following program (20 s at 500 rpm, 40 s at 1500 rpm, and 60 s at 2000 rpm). Then, the substrates were dried under vacuum for 2 h. PVA doped films were obtained by drop-casting of 200 μL of PVA doped solutions on borosilicate substrates (17.5 × 20 mm) leading to transparent film formation. Finally, the substrates were dried under vacuum for 2 h.

Flexible doped films were obtained following the same protocol except that the PVA doped solutions (1 mL) were deposited by drop-casting in a Teflon substrate (25 × 25 mm) and dried under vacuum at room temperature for 2 days. The thicknesses of the dried polymer films were measured using a profilometer. The thickness was measured at around 0.5 μm for spin-coated PMMA films and 100 μm for drop-casted PVA layer.

RESULTS AND DISCUSSION

Synthesis and Structure. The heteroleptic complexes $[Tb(\mathbf{L})(tfac)_2]$ (**1**) and $[Eu(\mathbf{L})(tta)_2]$ (**2**) were synthesized in good yield by reacting the $Tb(OTf)_3$ and $Eu(OTf)_3$ salts respectively first with the deprotonated ligand KL and then with the respective potassium β-diketonate ligands tfacK and ttaK as shown in Figure 1.

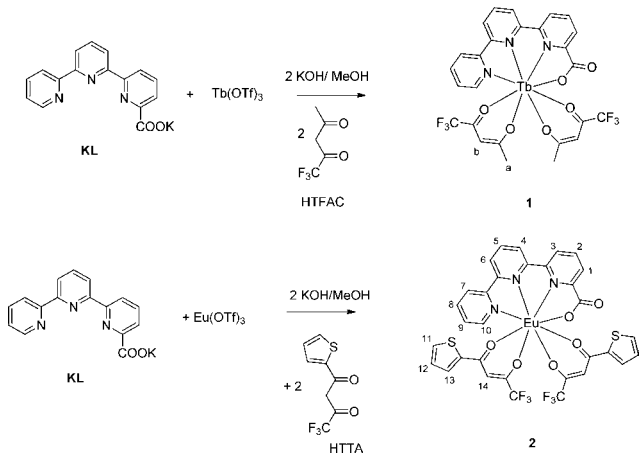

Figure 1. Synthesis of complexes **1** and **2**.

Single crystals suitable for X-ray diffraction were obtained for both complexes by slow evaporation of methanol solutions (Figure 2). Selected bond distances and angles are given in Table 1, while the full crystallographic data are presented in the Supporting Information, Tables S1 and S2.

The structures of the complexes **1**·MeOH and **2** were solved in the $P2_1/n$ space group of the monoclinic system and show the presence of neutral species. In the structure of **1**·MeOH

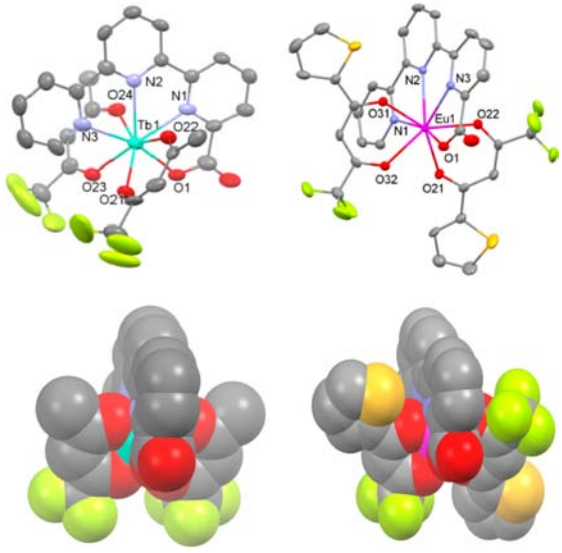

Figure 2. Ortep diagrams of the structure of complexes (**1**, top left and **2**, top right) and space-filled models (**1**, bottom left and **2**, bottom right). Thermal ellipsoids are at the 50% probability level (hydrogen atoms were omitted for clarity).

Table 1. Selected Bond Distances (Å) and Angles (deg) in 1·MeOH and 2

1		2	
Tb1–O1	2.297(7)	Eu1–O1	2.306(2)
Tb1–O23	2.339(6)	Eu1–O31	2.353(2)
Tb1–O22	2.345(7)	Eu1–O22	2.368(2)
Tb1–O21	2.328(7)	Eu1–O32	2.369(2)
Tb1–O24	2.356(6)	Eu1–O21	2.407(2)
Tb1–N1	2.457(8)	Eu1–N1	2.540(2)
Tb1–N2	2.536(7)	Eu1–N2	2.589(2)
Tb1–N3	2.514(8)	Eu1–N3	2.514(2)
N1–Tb1–N2	64.4(2)	N1–Eu1–N2	63.35(6)
N2–Tb1–N3	64.0(3)	N2–Eu1–N3	63.15(7)
O1–Tb1–N1	67.2(2)	O1–Eu1–N3	66.37(6)
O21–Tb1–O22	72.3(2)	O21–Eu1–O22	70.47(6)
O23–Tb1–O24	71.9(2)	O31–Eu1–O32	71.88(6)

two crystallographically independent complexes are found in the asymmetric unit. In both structures, the lanthanide ions are eight-coordinated, with slightly distorted dodecahedron geometry, by the four donor atoms of the terpyridine-carboxylate ligand and by four oxygen atoms from two β-diketonate ligands. No solvent molecules or water molecules are found in the first coordination sphere of the metal ions.

For the $[Eu(\mathbf{L})(tta)_2]$ complex, the Eu–O bond distances of the β-diketonate units (average 2.37(2) Å) are in the range of those found in other octa-coordinated tris-β-diketonate complexes containing bipyridine (mean Eu–O = 2.350 Å in $[Eu(tta)_3(bipy)]$)[56] or phenanthroline (mean Eu–O = 2.36(1) Å in $[Eu(tta)_3(phen)]$)[21,45] as a secondary ligand, and are similar to those found in the ternary nine-coordinated terpyridine complex $[Eu(DPM)_3(terpy)]$ with Eu–O = 2.38(3) Å (DPM = dipivaloylmethanate).[28] The value of the Eu–O bond distance is significantly shorter (2.306(2) Å) for the carboxylate moiety on the terpyridine. This value compares well with the mean Eu–$O_{carboxylate}$ distance found in the previously reported eigth-coordinated bis-ligand complex $[Eu(\mathbf{L})_2]OTf$ (2.31(1) Å).[42] The Eu–N bond distances

dx.doi.org/10.1021/ic402523v | Inorg. Chem. 2013, 52, 14382–14390

ranging from 2.514(2) to 2.589(2) Å are significantly shorter than the values found in the $[Eu(DPM)_3(terpy)]$ complex (with Eu−N distances between 2.612(5) and 2.680(5) Å)[28] but similar to those found in the $[Eu(\mathbf{L})_2]OTf$ complex (2.50−2.57 Å).[42]

The distances in $[Tb(\mathbf{L})(tfac)_2]$ present similar features, with a short Tb−O1 bond (2.297(7) Å) for the carboxylate moiety, and Tb−N bond distances ranging from 2.457(8) to 2.536(7) Å).

The terpyridine-carboxylate ring system is quasi-planar in both complexes (mean deviation from the plane = 0.07 Å; 0.04 Å; 0.18 Å in **2**, and in the two complexes in the structure of **1**, respectively) and the lanthanide ion is located within this plane. The β-diketonate ligands are found on the opposite sides of the plane defined by the terpyridine-carboxylate ligand. In the structure of $[Eu(\mathbf{L})(tta)_2]$, probably because of the larger size of the thiophene ring, the two β-diketonates are arranged antisymmetrically, with the CF_3 groups pointing in opposite directions, whereas in $[Tb(\mathbf{L})(tfac)_2]$, the arrangement of the two β-diketonates is symmetrical (CF_3 groups pointing in the same direction). The mean angles between each diketonate plane and the terpyridinecarboxylate plane are 112(1)° in **2** and 80(3)° in **1**.

The ^1H NMR spectrum of complex **1** in deuterated chloroform at 298 K is well resolved, and shows 10 signals with the same integration assigned to the 10 protons of the terpyridine ligand and four partially overlapped signals assigned to the 8 protons of the β-diketonate ligands. (Figure 3) These

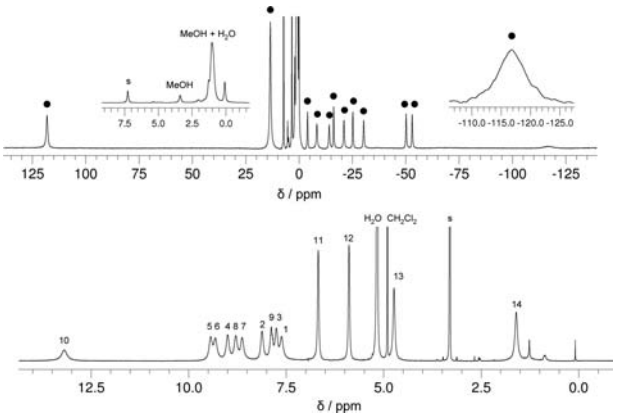

Figure 3. ^1H NMR spectrum of (top) **1** and (bottom) **2** in chloroform and methanol solution, at 298 and 268 K, respectively.

features are in agreement with the presence in solution of C_s symmetrical species having a symmetry plane passing through the terpyridine ligand which results in the two $tfac^-$ units being equivalent. The ^1H NMR spectrum of the complex **2** in methanol at room temperature shows 10 resonances which integrate for the 18 protons in the structure of the complex suggesting that the terpyridine signals are overlapped at 298 K. A variable temperature ^1H NMR experiment has been performed (Supporting Information, Figure S1). The NMR spectrum is better resolved at 268 K (Figure 3) showing 14 signals which have all been assigned by 2D ^1H-^1H COSY and NOESY experiments. These features are in agreement with the presence of dynamically averaged C_s symmetrical species in solution, where the two diketonate ligands are equivalent. Since the crystal structure of complex **2** does not present a pseudosymmetry plane passing through the **L** ligand, the proton NMR indicates the presence of a dynamic behavior in which the two diketonate ligands are involved in a fast exchange leading to a higher symmetry of the solution species compared to the solid state structure. Fast exchange of the diketonate ligand has been observed in other lanthanide ternary systems.[27]

The proton NMR spectra indicate that the heteroleptic complexes remain undissociated in methanol or chlorinated solvents and do not undergo ligand scrambling. The behavior of **2** toward hydrolysis has also been investigated by adding increasing amount of deuterated water in both MeOD and THF-d_6 solution of complex **2** (up to 30% of D_2O and following the evolution by NMR spectroscopy (v/v), Supporting Information, Figure S2). Addition of deuterated water induces a shift and a broadening of the ^1H signals suggesting that the water molecule might be entering the coordination sphere and/or rendering the coordination of the ligands more labile. However, the NMR spectrum in THF-d_6 solution in the presence of 30% D_2O do not show the presence of free terpyridine or β-diketonate ligands suggesting that these complexes are resistant with respect to ligand dissociation even in the presence of water.

UV−visible Absorption Properties. The UV−visible absorption properties of complexes **1** and **2** have been recorded in methanol solution (Figure 4 and Table 2).

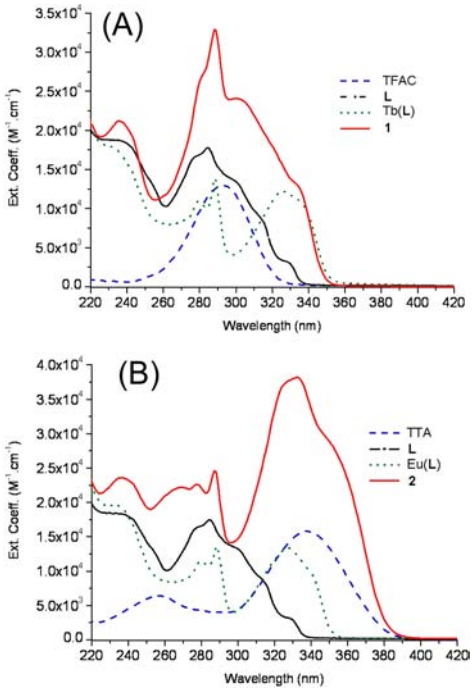

Figure 4. Absorption spectra of (A) deprotonated Ktfac and **1** and (B) K**L**, Ktta, and **2** in methanol at 298 K.

The absorption spectra of the ligands K**L** and β-diketonate, of the complexes **1** and **2** and of Eu**L** and Tb**L** (1:1 solutions of K**L** and of $Tb(OTF)_3$ and $Eu(OTf)_3$ salts in methanol) have been recorded in methanol and compared (Figure 4). Complex **1** presents a broad absorption band between 260 and 350 nm with a maximum in intensity at 289 nm and shoulders at 301 and 332 nm. In the case of **2**, the same large absorption band (300−390 nm) is observed, centered at 332 nm, with a shoulder at 350 nm. The potassium salts of the β-diketonate ligands (dashed lines) present mainly one absorption band (λ_{max} = 293 nm for Ktfac and 337 nm for Ktta) which has been

dx.doi.org/10.1021/ic402523v | Inorg. Chem. 2013, 52, 14382−14390

Table 2. Absorption Properties of Deprotonated Ligands and Complexes 1 and 2 in Methanol at 298 K

	λ_{abs}/nm ($\varepsilon \times 10^3$ M^{-1} cm^{-1})
Ktta	257 (6.4); 337 (15.8)
Ktfac	293 (13.1)
K**L**	235 (18.7); 284 (17.8); 298 (sh, 13.7); 312 (sh, 9.3); 329 (sh, 3.1)
[Tb(**L**)(tfac)$_2$]	236 (21.2); 280 (sh, 26.3); 289 (32.9); 301 (sh, 24.1); 332 (sh, 13.4)
[Eu(**L**)(tta)$_2$]	236 (23.6); 277 (22.6); 288 (24.6); 332 (38.2); 350 (sh, 28.8)

attributed previously to a singlet−singlet $\pi-\pi^*$ enolic transition. The bathochromic shift of the absorption maximum between Ktfac and Ktta is due to a higher conjugation path in the nonsymmetrical Ktta ligand. K**L** presents a broad composite absorption band between 260 and 340 nm (λ_{max} 323 nm) due to the aromatic core. It should be underlined that the introduction of the carboxylic acid onto the terpyridine unit induces a bathochromic shift of its absorption maximum by about 50 nm, from 280 to 330 nm.[57] Based on these observations, the most intense peaks for the terbium complex **1** at 289 and 301 nm are assigned to the overlapping absorption bands of both K**L** and Ktfac ligands. The shoulder observed at ∼332 nm in the spectrum of **1** is assigned to the LMCT terpyridine-Tb absorption transition. In the case of the europium complex **2**, the large absorption band arises from the overlap of the absorption of the β-diketonate ligand and of the LMCT absorption band of Eu**L**. The shoulder at 350 nm is now centered on the absorption of the Ktta diketonate. These data show that β-diketonate ligands can be used to tune the absorption wavelength in these ternary systems. This is particularly attractive for attaining absorption at lower energy required in many applications.

Ligand-Centered Luminescence. The lowest triplet states of the tta$^-$ and tfac$^-$ ligands have been previously reported and correspond to 488 and 420 nm, respectively.[47,58] The emission spectra of the ligand **L** and its nonluminescent gadolinium complex have been measured in methanol solutions at 298 K. UV excitation at 280 nm and at the maximum wavelength in the excitation spectra result in a ligand-centered emission displaying one asymmetric broad band assigned to the singlet state, with a maximum at 350 and 360 nm for the free ligand and its [Gd(**L**)$_2$]$^+$ complex, respectively (Supporting Information, Figure S3). At 77 K in methanol glass and upon enforcement of a time delay (0.2 ms), the singlet state emission disappears with concomitant appearance of a broad and structured band arising from the triplet state emission. The 0-phonon transition is located at 440 and 444 nm for the free ligand and its [Gd(**L**)$_2$]$^+$ complex, respectively.

These data indicate that in the ternary complex [Tb(**L**)(tfac)$_2$] (**1**) the sensitizing triplet state centered on the terpyridine acid ligand (440 nm) is close in energy to both the lowest triplet state of the tfac$^-$ ligand (420 nm) and the Tb^{3+} emissive $^5D_4$ level (480 nm). Thus back energy transfer should play an important role in the sensitization process which is consistent with a relatively short lifetime of the Tb($^5D_4$) level. In the case of [Eu(**L**)(tta)$_2$] (**2**), the lowest triplet state should be located on the tta$^-$ ligand (488 nm) which lies above the first excited state of Eu^{3+} ion ($^5D_0$ at 580 nm) with an energy gap allowing an efficient ligand to metal energy transfer.

Metal Centered Luminescence. Excitation spectra of **1** recorded in solid state upon monitoring the $^7F_5$ transition (Figure 5) present a band between 280 and 450 nm. Upon excitation of complex [Tb(**L**)(tfac)$_2$] through the ligand levels

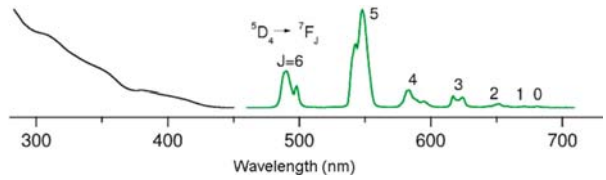

Figure 5. Excitation (λ_{an} = 545 nm, left) and emission (λ_{exc} = 380 nm, right) spectra of **1** in solid state at 298 K.

(380 nm), the characteristic $^5D_4 \rightarrow {}^7F_J$ transitions (J = 0−6) are observed and dominated by the very intense $^7F_5$ transition. Moreover, the ligand-centered emission is not detected pointing to an efficient ligand to metal energy transfer process.

The luminescence decay of the [Tb(**L**)(tfac)2] complex has been fitted to a monoexponential function yielding a value of the luminescence lifetime of 0.34 ms (Table 3) with a quantum yield measured in the solid state at 13(1)%.

Table 3. Photophysical Properties for 1 and 2

cpd.		λ_{max}/nm	τ/ms	Φ/%
1	solid	380	0.34(2)	13(1)
2	solid	370	0.79(4)	66(6)
	anhydrous THF		0.72(3)	54(5)
	THF + 30% H_2O		0.43(4)	27(3)
	THF + 30% D_2O		0.64(3)	
	MeOH		0.52(2)	23(2)
	MeOD		0.70(3)	
	MeOH + 30% H_2O		0.38(2)	13(1)

The short lifetime is explained by a partial back-energy transfer from the triplet state of both tfac$^-$ and **L** ligands to the Tb ($^5D_4$) emissive state, which also results in a lower quantum yield compared to the bis-aqua complex [Tb(tfac)$_3$(H$_2$O)$_2$] ((27(3)%).[30,59] Since the value of the solid state luminescence quantum yield of **1** is quite low we have not investigated further the properties of this complex.

Excitation spectra of **2** recorded in solid state and in solution upon monitoring the $^7F_2$ transition (Figure 6) showed the same broad maxima at around 370−380 nm. The observed hypsochromic shift observed in solution with respect to the solid state is probably due to the presence of strong $\pi-\pi$ interactions in the solid state structure of **2** that are disrupted in solution. Upon excitation through the ligand levels (370 nm), the characteristic $^5D_0 \rightarrow {}^7F_J$ (J = 0−4) transitions are observed, and they are dominated by a very intense $^7F_2$ band, indicating a high level of red color purity. Either in solution or in solid state, the ligand-centered emission is not detected pointing to an efficient ligand to metal energy transfer process. Furthermore, the emission spectra show the same transitions and splitting in both solution and solid state, pointing to a very similar structure in solution. These results highlight the interest of using the tetradentate ligand **L** as a cosensitizer ligand to afford robust ternary β-diketonates complexes that do not undergo partial ligand-decomplexation. This is particularly desirable for the easy and reproducible handling of such compounds in practical applications. The value of the absolute luminescence quantum yield in the solid state is very high at 66%. Only a

dx.doi.org/10.1021/ic402523v | Inorg. Chem. 2013, 52, 14382−14390

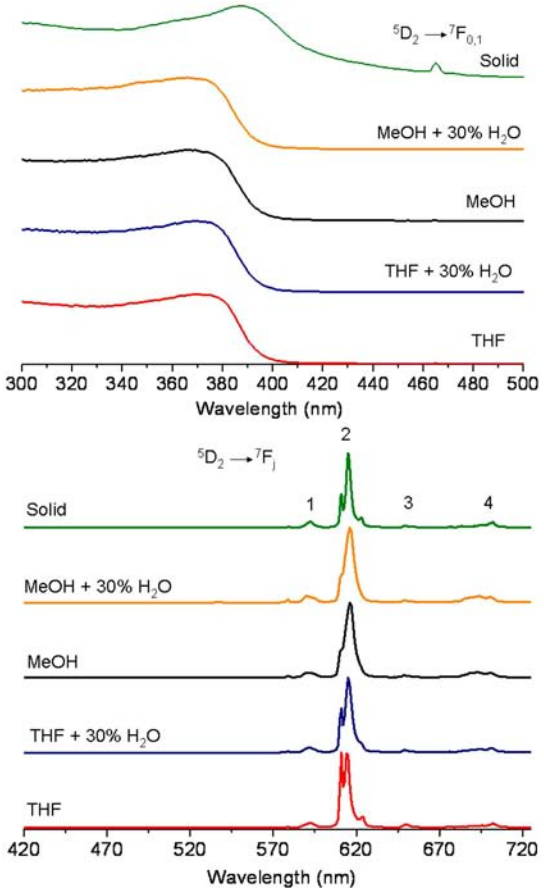

Figure 6. Excitation (λ_{an} = 615 nm, up) and emission (λ_{exc} = 370 nm, down) spectra of **2** in solid state and 1 mM solution at 298 K.

small decrease is observed in anhydrous THF solution (54%) while a lower value is measured in methanol (23%) (Table 3).

The luminescence decays of the $[Eu(\mathbf{L})(tta)_2]$ emission, measured at the $^7F_2$ site upon ligand excitation, can be fitted to a monoexponential function affording a value of the luminescence lifetime of 0.79 ms in the solid state at 298 K. This value indicates the absence of solvent molecules in the first coordination sphere of the metal, in agreement with the X-ray structure. The luminescence lifetime of **2** has a similar value in anhydrous THF solution but decreases in methanol to 0.52 ms. The number of coordinated methanol molecules (q) has been determined by recording the excited lifetime in methanol-d_1 (MeOD) using eq 2[60]

$$q = 2.1(\tau^{-1}{}_{MeOH} - \tau^{-1}{}_{MeOD}) \quad (2)$$

where τ^{-1} is the reciprocal excited-state lifetime, taken separately in the nondeuterated and deuterated solvent. The q value has been found to be equal to 1.0 indicating the coordination of one methanol molecule in methanol solution. Thus the presence of coordinated methanol is probably the cause of the decrease in the luminescence lifetime and luminescence quantum yield through nonradiative deactivation in methanol solution.

To investigate the stability of complex **2** in solution with respect to ligand dissociation, photophysical studies have also been carried out in the presence of 30% H_2O in methanol and THF solution (Figure 6). Addition of water does not affect the excitation spectra of complex **2** and only a slight broadening of the $^7F_2$ emission band is observed in the emission spectra. No ligand centered emission band is observed in the presence of water. The luminescence quantum yield and luminescence lifetimes are clearly affected by the introduction of water in solution since they decrease by almost a factor two in THF/water and methanol/water solutions (Table 3). The number of coordinated water molecules (q) has been determined by recording the excited lifetime in THF/30% D_2O mixture using eq 3.[61]

$$q = 1.05(\tau^{-1}{}_{H2O} - \tau^{-1}{}_{D2O}) \quad (3)$$

The q value has been found to amount to 0.8 indicating the presence of one coordinated water molecule in THF. These results suggest that ligand dissociation does not occur in the conditions used in the luminescence experiments but that in the presence of protic solvents such as methanol or water, the coordination of one solvent molecule occurs resulting in a decrease of the luminescence quantum yields as they are both vibrational deactivators of the excited states of Ln^{3+} ions.

Incorporation of $[Eu(L)(tta)_2]$ in PMMA and PVA. For potential applications of lanthanide complexes as light emitters or converters, high quantum yields combined with a large excitation window are required. The optical properties of complex $[Eu(\mathbf{L})(tta)_2]$ and its stability make it a suitable candidate for technological applications. We have also investigated the film-forming properties of **2** by dispersing it in widely used polymer matrixes such as PMMA and PVA.

PMMA, a low-cost material possessing high transparency and adequate resistance to heat, is one of the most popular polymer matrixes for these applications.[14,62,63] On the other hand, PVA presents better mechanical properties that are of interest for the development of flexible films for large-area optoelectronic devices.[64]

PMMA and PVA films doped with $[Eu(\mathbf{L})(tta)_2]$ have been prepared by dissolving PMMA or PVA in THF (5 and 10%, w/w respectively) in the presence of different concentration of complex **2** (from 1 to 5 mM). Polymeric transparent sheets and films doped with $[Eu(\mathbf{L})(tta)_2]$ have been obtained by spin-coating (PMMA) or drop-casting (PVA) on glass substrates, and their photophysical properties have been investigated on glass substrates.

Absorption spectra of $[Eu(\mathbf{L})(tta)_2]$ in either PMMA and PVA matrix on glass substrates match perfectly those obtained in solution, suggesting a similar molecular structure of **2** when embedded in the host matrix (Figure 7). Thus visible excitation is obtained through ligand excitation up to 390 nm even on glass substrate.

Excitation spectra of doped film monitored at the $^5D_0 \rightarrow {}^7F_2$ transition at 612 nm show a broad band between 300 and 390 nm corresponding to both the absorption and the excitation spectra of $[Eu(\mathbf{L})(tta)_2]$ in THF and in solid state respectively (Figure 7 and 8). This observation confirmed that sensitization of europium emission occurs through energy transfer from the ligand states for the complex embedded in the polymer matrixes. Upon ligand excitation at 335−385 nm, the $^5D_0 \rightarrow {}^7F_J$ (J = 0−4) typical Eu^{3+} emission bands are observed, the $^5D_0 \rightarrow {}^7F_2$ being the most intense with an efficient ligand-to-metal energy-transfer process ($^3\pi-\pi^*$ emission not detected).

The luminescence decays of $[Eu(\mathbf{L})(tta)_2]$ emission incorporated into polymer matrixes, measured on the $^7F_2$ transition (615 nm) upon ligand excitation (370 nm), can be fitted as a monoexponential function and yield a lifetime of 0.73 and 0.76 ms for PMMA and PVA, respectively (Table 4). These

dx.doi.org/10.1021/ic402523v | Inorg. Chem. 2013, 52, 14382−14390

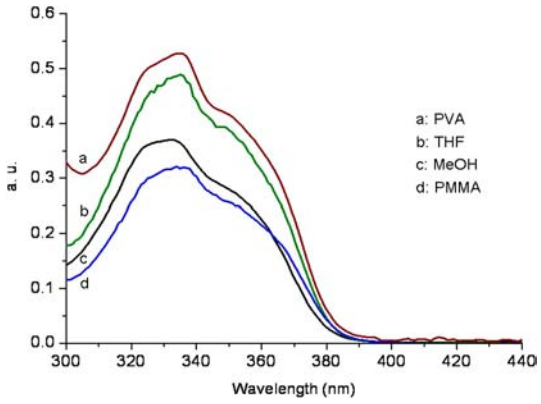

Figure 7. Absorption properties of **1** in solvents and polymers.

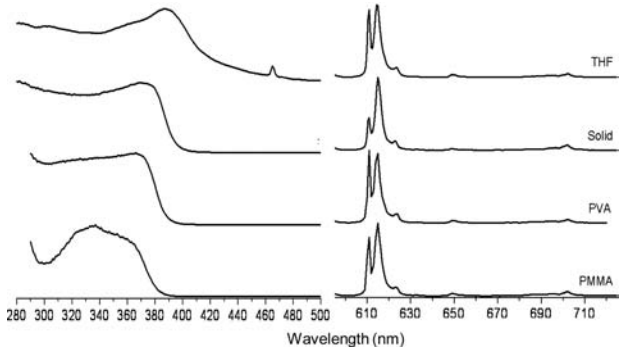

Figure 8. Excitation (left) and emission (right) spectra of polymeric Eu-doped films on glass substrate.

Table 4. Photophysical Properties for 2 in Polymeric Matrixes at 298 K

complex	matrix	λ_{max}/nm	τ/ms	Φ/%
2	PMMA 5%	370	0.73(3)	62(6)
	PVA 10%		0.76(4)	60(6)

values are in accordance with those found for **2** in solid state (0.79 ms), showing that the host matrixes do not interact with the complex and have no influence on the sensitization process of the lanthanide ion. Moreover, the high absolute luminescence quantum yield of the complex is maintained (within the experimental error of 10%) in the different polymer hosts amounting to 62 and 60% in PMMA and PVA, respectively, compared to 66% measured for **2** in the solid state. These luminescence quantum yield values are significantly higher than the values reported for the bis-aqua complex $[Eu(H_2O)_2(tta)_3]$ in solid state (29%)[65] or in PMMA (47%)[49] and similar to those measured for the $[Eu(tta)_3(phen)]$ complex in PMMA (72%).[20]

More interestingly, when the PVA doped layers are prepared starting from a solution of the complex in a THF/30% H_2O mixture using the same experimental protocol, the luminescence properties of the resulting doped polymer remain unchanged. Thus the luminescence quantum yield of the complex is improved (60% with a luminescence lifetime of 0.74 ms) compared to the value measured in THF/30% H_2O (27(3)%) by imbedding in the PMMA or PVA polymer. This increase in quantum yield is assigned to the replacement of coordinated water molecules by the C=O groups present in the structure of the PMMA and PVA polymers. Enhancement of the luminescence quantum yield of aqua complexes after embedding in a polymeric matrix (poly-β-hydroxybutyrate) presenting coordinating carbonyl groups has been previously reported.[66]

The drop casting technique affords higher thickness compared to spin-coating techniques, and Figure 9 presents

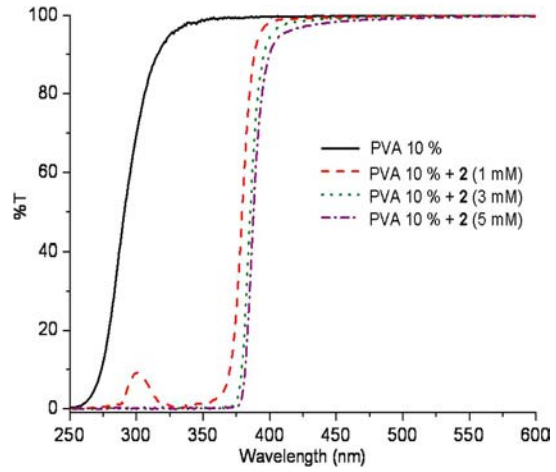

Figure 9. Transmission spectra of PVA doped films with **2**.

the transmission properties of PVA doped films on glass substrates with increasing concentration of complex **2**. The entire incident light is absorbed from 250 to 380 nm by increasing the complex concentration without any losses of transparency up to 400 nm. The high light absorption and high luminescence quantum yield renders these europium doped polymer suitable candidates for application as a light down-shifting layer in solar cells.[4]

Finally, to highlight the use of these materials for flexible displays, we have prepared flexible PVA doped films using a solution of PVA containing 1 mM of complex **2**. Upon excitation at 365 nm, the characteristic red emission of europium can be observed (Figure 10). This preliminary study illustrates the potentialities of our complexes for the preparation of highly luminescent flexible plastics.

CONCLUDING REMARKS

A new type of robust ternary complexes of europium and terbium have been prepared from the reaction of Eu(III) and Tb(III) ions with two β-diketonates ligands and one terpyridine-carboxylate ligand. The solid state structure of the two complexes $[Tb(\mathbf{L})(tfac)_2]$ (**1**) and $[Eu(\mathbf{L})(tta)_2]$ (**2**)

Figure 10. Picture of flexible PVA doped film excited with UV lamp.

dx.doi.org/10.1021/ic402523v | Inorg. Chem. 2013, 52, 14382−14390

shows the absence of water molecules coordinated to the metal center. Photophysical and ^{1}H NMR indicate a high stability of these complexes with respect to ligand dissociation in solution. The use of the anionic tetradentate ligand in combination with two β-diketonates units leads to the extension of the absorption window toward the visible region (390 nm) and to high luminescence quantum yield for the europium complex in the solid state (Φ= 66%). This high value of the luminescence quantum yield is retained in non protic solvents, but the presence of coordinating water molecules leads to partial deactivation of the luminescence emission. However, the high value of the luminescence quantum yield is restored (60%) when the europium complex is embedded in the polymeric matrixes PVA or PMMA. Moreover, the observed stability of the ternary complexes with respect to ligand dissociation allows the preparation of the films in nonanhydrous conditions. As such the europium complex reported here is a promising candidate for practical application in OLED emitting layers and solar concentrators.

■ ASSOCIATED CONTENT

Ⓢ Supporting Information

Selected ^{1}H NMR spectra, X-ray crystallographic data and files in CIF format. This material is available free of charge via the Internet at http://pubs.acs.org.

■ AUTHOR INFORMATION

Corresponding Author

*E-mail: marinella.mazzanti@cea.fr.

Author Contributions

All authors have given approval to the final version of the manuscript.

Notes

The authors declare no competing financial interest.

■ ACKNOWLEDGMENTS

E.S.A. was supported by the European Community under the FP6 Marie Curie Host Fellowships for EST "CHEMTRONICS" MEST-CT-2005-020513. N.G. thanks the Nanoscience foundation and Chimtronic research program (6.3.8 ConvSpec) for financial support. The Labex Arcane, ANR-11-LABX-003-01, is gratefully acknowledged.

■ REFERENCES

(1) de Sa, G. F.; Malta, O. L.; Donega, C. D.; Simas, A. M.; Longo, R. L.; Santa-Cruz, P. A.; da Silva, E. F. *Coord. Chem. Rev.* **2000**, *196*, 165−195.

(2) Binnemans, K. In *Handbook on the Physics and Chemistry of Rare Earths*; Gschneidner, K. A., Jr.; Bünzli, J. C. G. , Pecharsky, V. K., Eds.; Elsevier: Amsterdam, The Netherlands, 2005; Vol. *35*, pp 107−272.

(3) Binnemans, K. *Chem. Rev.* **2009**, *109*, 4283−4374.

(4) Bünzli, J. C. G.; Eliseeva, S. V. *Chem. Sci.* **2013**, *4*, 1939−1949.

(5) Eliseeva, S. V.; Bünzli, J. C. G. *Chem. Soc. Rev.* **2010**, *39*, 189−227.

(6) Xin, H.; Li, F. Y.; Shi, M.; Bian, Z. Q. A.; Huang, C. H. *J. Am. Chem. Soc.* **2003**, *125*, 7166−7167.

(7) de Bettencourt-Dias, A. *Dalton Trans.* **2007**, 2229−2241.

(8) Kido, J.; Okamoto, Y. *Chem. Rev.* **2002**, *102*, 2357−2368.

(9) Katkova, M. A.; Bochkarev, M. N. *Dalton Trans.* **2010**, *39*, 6599−6612.

(10) Chen, X. Y.; Yang, X.; Holliday, B. J. *J. Am. Chem. Soc.* **2008**, *130*, 1546−1547.

(11) Huang, X. Y.; Han, S. Y.; Huang, W.; Liu, X. G. *Chem. Soc. Rev.* **2013**, *42*, 173−201.

(12) Le Donne, A.; Acciarri, M.; Narducci, D.; Marchionna, S.; Binetti, S. *Prog. Photovoltaics* **2009**, *17*, 519−525.

(13) Graffion, J.; Cattoen, X.; Man, M. W. C.; Fernandes, V. R.; Andre, P. S.; Ferreira, R. A. S.; Carlos, L. D. *Chem. Mater.* **2011**, *23*, 4773−4782.

(14) Moudam, O.; Rowan, B. C.; Alamiry, M.; Richardson, P.; Richards, B. S.; Jones, A. C.; Robertson, N. *Chem. Commun.* **2009**, 6649−6651.

(15) Wang, X.; Wang, T. X.; Tian, X. J.; Wang, L. J.; Wu, W. X.; Luo, Y. H.; Zhang, Q. J. *Sol. Energy* **2011**, *85*, 2179−2184.

(16) Eliseeva, S. V.; Bünzli, J. C. G. *New J. Chem.* **2011**, *35*, 1165−1176.

(17) Bourdolle, A.; Allali, M.; D'Aleo, A.; Baldeck, P. L.; Kamada, K.; Williams, G. J. H.; Le Bozec, H.; Andraud, C.; Maury, O. *ChemPhysChem* **2013**, 3361−3367.

(18) Hu, Z. J.; Tian, X. H.; Zhao, X. H.; Wang, P.; Zhang, Q.; Sun, P. P.; Wu, J. Y.; Yang, J. X.; Tian, Y. P. *Chem. Commun.* **2011**, *47*, 12467−12469.

(19) Lo, W. S.; Kwok, W. M.; Law, G. L.; Yeung, C. T.; Chan, C. T. L.; Yeung, H. L.; Kong, H. K.; Chen, C. H.; Murphy, M. B.; Wong, K. L.; Wong, W. T. *Inorg. Chem.* **2011**, *50*, 5309−5311.

(20) Wong, K. L.; Law, G. L.; Kwok, W. M.; Wong, W. T.; Phillips, D. L. *Angew. Chem., Int. Ed.* **2005**, *44*, 3436−3439.

(21) Freund, C.; Porzio, W.; Giovanella, U.; Vignali, F.; Pasini, M.; Destri, S.; Mech, A.; Di Pietro, S.; Di Bari, L.; Mineo, P. *Inorg. Chem.* **2011**, *50*, 5417−5429.

(22) Biju, S.; Raj, D. B. A.; Reddy, M. L. P.; Kariuki, B. M. *Inorg. Chem.* **2006**, *45*, 10651−10660.

(23) Zucchi, G.; Murugesan, V.; Tondelier, D.; Aldakov, D.; Jeon, T.; Yang, F.; Thuery, P.; Ephritikhine, M.; Geffroy, B. *Inorg. Chem.* **2011**, *50*, 4851−4856.

(24) Eliseeva, S. V.; Pleshkov, D. N.; Lyssenko, K. A.; Lepnev, L. S.; Bünzli, J. C. G.; Kuzmina, N. P. *Inorg. Chem.* **2011**, *50*, 5137−5144.

(25) Raj, D. B. A.; Francis, B.; Reddy, M. L. P.; Butorac, R. R.; Lynch, V. M.; Cowley, A. H. *Inorg. Chem.* **2010**, *49*, 9055−9063.

(26) He, G. J.; Guo, D.; He, C.; Zhang, X. L.; Zhao, X. W.; Duan, C. Y. *Angew. Chem., Int. Ed.* **2009**, *48*, 6132−6135.

(27) Zaim, A.; Nozary, H.; Guenee, L.; Besnard, C.; Lemonnier, J. F.; Petoud, S.; Piguet, C. *Chem.—Eur. J.* **2012**, *18*, 7155−7168.

(28) Holz, R. C.; Thompson, L. C. *Inorg. Chem.* **1988**, *27*, 4640−4644.

(29) Yang, C.; Fu, L.-M.; Wang, Y.; Zhang, J.-P.; Wong, W.-T.; Ai, X.-C.; Qiao, Y.-F.; Zou, B.-S.; Gui, L.-L. *Angew. Chem., Int. Ed.* **2004**, *43*, 5010−5013.

(30) Eliseeva, S. V.; Kotova, O. V.; Gumy, F.; Semenov, S. N.; Kessler, V. G.; Lepnev, L. S.; Bünzli, J. C. G.; Kuzmina, N. P. *J. Phys. Chem. A* **2008**, *112*, 3614−3626.

(31) Lemonnier, J. F.; Babel, L.; Guenee, L.; Mukherjee, P.; Waldeck, D. H.; Eliseeva, S. V.; Petoud, S.; Piguet, C. *Angew. Chem., Int. Ed.* **2012**, *51*, 11302−11305.

(32) Stanley, J. M.; Zhu, X. J.; Yang, X. P.; Holliday, B. J. *Inorg. Chem.* **2010**, *49*, 2035−2037.

(33) Kadjane, P.; Charbonniere, L.; Camerel, F.; Laine, P. P.; Ziessel, R. *J. Fluoresc.* **2008**, *18*, 119−129.

(34) Nockemann, P.; Beurer, E.; Driesen, K.; Van Deun, R.; Van Hecke, K.; Van Meervelt, L.; Binnemans, K. *Chem. Commun.* **2005**, 4354−4356.

(35) Biju, S.; Gopakumar, N.; Bünzli, G. J.-C.; Scopeliti, R.; Kim, H. K.; Reddy, M. L. P. *Inorg. Chem.* **2013**, *52*, 8750−8758.

(36) Chauvin, A. S.; Gumy, F.; Matsubayashi, I.; Hasegawa, Y.; Bünzli, J. C. G. *Eur. J. Inorg. Chem.* **2006**, 473−480.

(37) Zaim, A.; Dalla Favera, N.; Guenee, L.; Nozary, H.; Hoang, T. N. Y.; Eliseeva, S. V.; Petoud, S.; Piguet, C. *Chem. Sci.* **2013**, *4*, 1125−1136.

(38) Andreiadis, E. S.; Imbert, D.; Pecaut, J.; Demadrille, R.; Mazzanti, M. *Dalton Trans.* **2012**, *41*, 1268−1277.

(39) Giraud, M.; Andreiadis, E. S.; Fisyuk, A. S.; Demadrille, R.; Pecaut, J.; Imbert, D.; Mazzanti, M. *Inorg. Chem.* **2008**, *47*, 3952−3954.

(40) Andreiadis, E. S.; Demadrille, R.; Imbert, D.; Pecaut, J.; Mazzanti, M. *Chem.—Eur. J.* **2009**, *15*, 9458−9476.
(41) Chen, X. Y.; Bretonniere, Y.; Pecaut, J.; Imbert, D.; Bünzli, J. C.; Mazzanti, M. *Inorg. Chem.* **2007**, *46*, 625−637.
(42) Bretonniere, Y.; Mazzanti, M.; Pecaut, J.; Olmstead, M. M. *J. Am. Chem. Soc.* **2002**, *124*, 9012−9013.
(43) Shavaleev, N. M.; Eliseeva, S. V.; Scopelliti, R.; Bünzli, J. C. G. *Inorg. Chem.* **2010**, *49*, 3927−3936.
(44) Shavaleev, N. M.; Eliseeva, S. V.; Scopelliti, R.; Bünzli, J. C. G. *Chem.—Eur. J.* **2009**, *15*, 10790−10802.
(45) De Silva, C. R.; Maeyer, J. R.; Wang, R. Y.; Nichol, G. S.; Zheng, Z. *Inorg. Chim. Acta* **2007**, *360*, 3543−3552.
(46) Malta, O. L.; Brito, H. F.; Menezes, J. F. S.; Silva, F.; Alves, S.; Farias, F. S.; deAndrade, A. V. M *J. Lumin.* **1997**, No. 75, 255−268.
(47) Zheng, Y. X.; Lin, J.; Liang, Y. J.; Lin, Q.; Yu, Y. N.; Meng, Q. G.; Zhou, Y. H.; Wang, S. B.; Wang, H. Y.; Zhang, H. J. *J. Mater. Chem.* **2001**, *11*, 2615−2619.
(48) Klampaftis, E.; Congiu, M.; Robertson, N.; Richards, B. S. *IEEE J. Photovoltaics* **2011**, *1*, 29−36.
(49) Kai, J. A.; Felinto, M.; Nunes, L. A. O.; Malta, O. L.; Brito, H. F. *J. Mater. Chem.* **2011**, *21*, 3796−3802.
(50) Schwarzenbach, G. *Complexometric Titrations*; Chapman &Hall: London, U.K., 1957.
(51) *CrysAlis PRO*; Agilent Technologies: Yarnton, England, 2010.
(52) *CrysAlisPro CCD; CrysAlisPro RED; ABSPACK; CrysAlis PRO*; Agilent Technologies: Yarnton, England, 2010.
(53) Sheldrick, G. M. *SHELXTL* 6.14 ed.; University of Göttingen: Göttingen, Germany, 2006.
(54) *Origin8*; OriginLabCorp: Northampton, MA, 2008.
(55) Jameson, D. L.; Guise, L. E. *Tetrahedron Lett.* **1991**, *32*, 1999−2002.
(56) Chen, X.-F.; Zhu, X.-H.; Xu, Y.-H.; Shanmuga Sundara Raj, S.; Ozturk, S.; Fun, H.-K.; Ma, J.; You, X.-Z. *J. Mater. Chem.* **1999**, *9*, 2919−2922.
(57) Albano, G.; Balzani, V.; Constable, E. C.; Maestri, M.; Smith, D. R. *Inorg. Chim. Acta* **1998**, *277*, 225−231.
(58) Kim, H. J.; Lee, J. E.; Kim, Y. S.; Park, N. G. *Opt. Mater.* **2002**, *21*, 181−186.
(59) Eliseeva, S. V.; Ryazanov, M.; Gumy, F.; Troyanov, S. I.; Lepnev, L. S.; Bünzli, J. C. G.; Kuzmina, N. P. *Eur. J. Inorg. Chem.* **2006**, 4809−4820.
(60) Holz, R. C.; Chang, C. A.; Horrocks, W. D. *Inorg. Chem.* **1991**, *30*, 3270−3275.
(61) Horrocks, W. D., Jr.; Sudnick, D. R. *J. Am. Chem. Soc.* **1979**, *101*, 334−340.
(62) Singh, A. K.; Singh, S. K.; Mishra, H.; Prakash, R.; Rai, S. B. *J. Phys. Chem. B* **2010**, *114*, 13042−13051.
(63) Raj, D. B. A.; Francis, B.; Reddy, M. L. P.; Butorac, R. R.; Lynch, V. M.; Cowley, A. H. *Inorg. Chem.* **2010**, *49*, 9055−9063.
(64) Shahi, S. *Nat. Photonics* **2010**, *4*, 506−506.
(65) Malta, O. L.; Brito, H. F.; Menezes, J. F. S.; Silva, F.; Donega, C. D.; Alves, S. *Chem. Phys. Lett.* **1998**, *282*, 233−238.
(66) Biju, S.; Reddy, M. L. P.; Cowley, A. H.; Vasudevan, K. V. *J. Mater. Chem.* **2009**, *19*, 5179−5187.